

# Single Plane Radial, Magnetic Bearings Biased With Poles Containing Permanent Magnets

**Andrew Kenny**

e-mail: a-kenny@tamu.edu

**Alan B. Palazzolo**

Mem. ASME

e-mail: a-palazzolo@tamu.edu

Vibration Control and Electromechanics  
Laboratory,  
Department of Mechanical Engineering,  
Texas A&M University  
College Station, TX 77845

*Magnetic bearings biased with permanent magnets have lower coil resistance power losses, and the magnets can also be used to help support a constant side load. In this paper, the performance of a single plane radial magnetic bearing biased with permanent magnets in several poles is presented. Although it has less load capacity and stiffness than a similarly sized electrically biased single plane heteropolar bearing, it does not require bias current, and its ratio of load capacity to coil resistance power loss is significantly better. This type of permanent magnet bearing has only a single plane of poles. It can be distinguished from the homopolar bearing type which has two planes and which can also be biased with permanent magnets. Magnetic circuit models for the novel single plane bearing are presented along with verification by finite element models. Equations for the key performance parameters of load capacity, stiffness, coil inductance and resistive power loss are also presented. [DOI: 10.1115/1.1541630]*

## 1 Introduction

Radial magnetic bearings are used to suspend rotors in many types of machines. These types of bearings have the advantage that they can be used to actively control the rotor vibration as well as support a steady load. Magnetic bearings are actually complex systems including an electromechanical actuator with sensors, a power amplifier, and an electronic controller [1]. The characteristics of two types of magnetic bearings have been described in the literature. These are heteropolar bearings which use electric current for bias and homopolar bearings which can use either electric bias or permanent magnet bias.

Previous papers on permanent magnet biased magnetic bearings have covered the characteristics of the coplanar geometry. One of the earliest descriptions of this geometry, usually called the homopolar design, was by Meeks [2]. These bearings may have either a permanent magnet in the backiron or an electric coil to provide the bias flux for two parallel stators. Sortore et al. published experimental results verifying the relatively low amount of electrical power required by homopolar bearings biased with permanent magnets [3].

Permanent magnet bias reduces the amount of current required for magnetic bearing operation. This reduces the power lost due to the coil current resistance. Coil current resistive losses not only reduce the bearing efficiency, but the heat produced is also a major design consideration. Nataraj and Calvert considered this in detail and gave convection and conduction coefficients to aid in the design of magnetic bearings [4]. Grbesa presented an efficient homopolar bearing with three poles per plane [5]. Saari and Lindgren analyzed the efficiency of an electrically biased heteropolar bearing [6]. Kasarda et al. examined the power losses due to the rotating conductor effect in both heteropolar and homopolar bearings [7].

Lee, Hsiao, and Ko derived detailed equations for predicting the flux in the major paths of a homopolar bearing. They described how to calculate the flux produced by the permanent magnet, and presented an advanced circuit model for these type of bearings and derived equations for the load capacity, current stiffness, and displacement stiffness [8]. Fan, Lee, and Hsiao then published a methodology for the design of these types of bearings [9].

Overstreet, Flowers, and Szasz described an advanced homopolar bearing design using four separate permanent magnets. They presented measured test results on the bearing load capacity up to and even past the magnetic flux saturation threshold [10]. Fukata, Yutani, and Kouya derived equations and provided corresponding experimental results for the dynamic motion of a rotor suspended by a homopolar bearing [11].

Jagannathan used one dimensional circuit analysis and described the design of an electrically biased heteropolar bearing [12]. Schmidt, Platter, and Springer compared heteropolar bearing parameters which they derived from an enhanced circuit model, to those they calculated from a finite element model. They found the finite element method was superior for the case where the rotor was significantly offset from the center [13]. Rockwell, Allaire, and Kasarda described a finite element model which also included the effect of rotor motion [14].

Imlach, Blair, and Allaire presented a comparison between the measured and predicted force and stiffness characteristics [15]. Measurements including the effects of hysteresis and frequency response for the force versus coil current in a heteropolar bearing were reported by Fitro, Baun, Maslen, and Allaire [16].

This paper is focused on a certain type of single plane bearing biased with permanent magnets in the poles. Others, such as Masayuk [17], and Nagaghiko [18] have proposed bearings with magnets in the poles. However, the bearing that is presented here is different in that the poles with permanent magnets are designed solely for supplying the bias flux. Maslen et al. presented a two plane homopolar bearing where one of the planes was used solely for providing bias flux [19]. Lewis, D. W., Humphris, R. R., Maslen, E. H., and Williams [20], and Yamauchi and Kuwahara [21], have presented a different type of single plane bearing biased with permanent magnets between each stator C core. In this paper, the performance equations are derived for a single plane bearing with bias only poles. The method of magnetic circuits, as described by Woodson and Melcher, is used to calculate the flux in air gaps [22]. The bearings are also analyzed with finite element models which have the advantage of including 3-D effects [23,24].

The innovative permanent magnet biased heteropolar magnetic bearing, (BPB, bias pole bearing), introduced here avoids some key drawbacks of both heteropolar and homopolar designs while retaining some of their advantageous features. To illustrate:

(a) The BPB only requires flux to flow in the plane of the laminate stack. The homopolar MB requires cross laminate flux

Contributed by the Reliability Stress Analysis and Failure Prevention, Committee for publication in the JOURNAL OF MECHANICAL DESIGN. Manuscript received April 2001; revised April 2002. Associate Editor: J. Vance.

flow and bias flux flow through a possibly unlaminated rotor return path. This causes increased bias flux reluctance due to the stacking factor effect and possibly eddy current generation with its accompanying heat and drag torque [25].

(b) The BPB bias flux is produced passively there by eliminating the  $I_{bias}^2 R$  losses inherent in conventional heteropolar bearings.

(c) The BPB may be easier to design or build than the homopolar bearing which requires a detailed examination of leakage between the two axial planes, stacking factor reluctance effects, possible recirculation of bias flux within the permanent magnet and consequent segmenting requirements.

(d) The BPB may require a shorter length than the homopolar bearing because of its single plane construction.

The BPB does have north—south flux reversals for the rotor material which may encounter higher hysteresis losses and eddy current losses than a homopolar design. Thus in total, this bearing provides a compromise between the homopolar and heteropolar approaches.

## 2 Bearing Structure

The bearing for which the magnetic circuit and performance equations will be presented is a single plane bearing where permanent magnet poles are dedicated solely to providing a bias flux. A high reluctance permanent magnet and large air gap prevent control flux from flowing through these bias poles. The bias poles

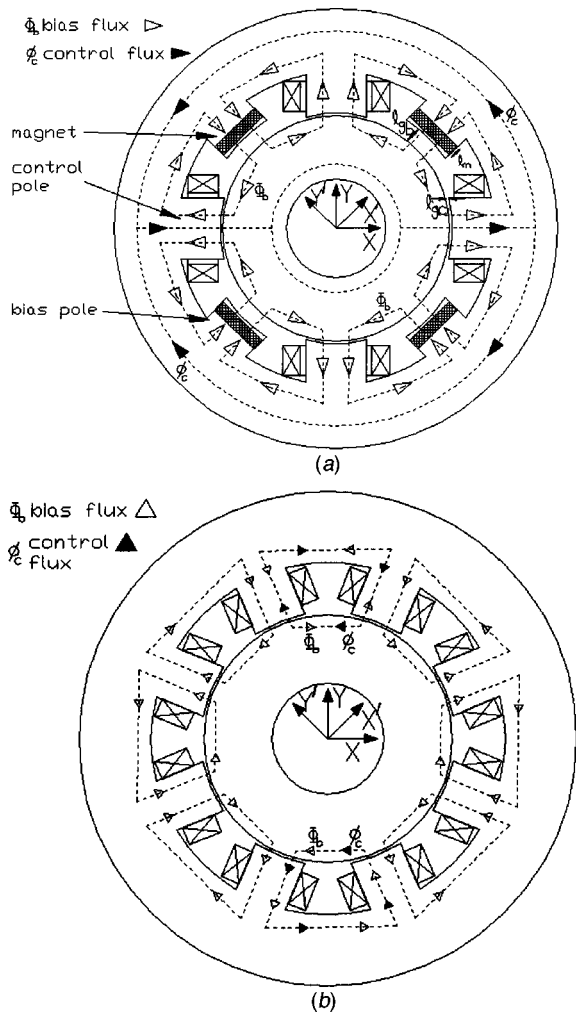


Fig. 1 (a) Eight pole symmetric bias pole bearing, and (b) eight pole heteropolar bearing

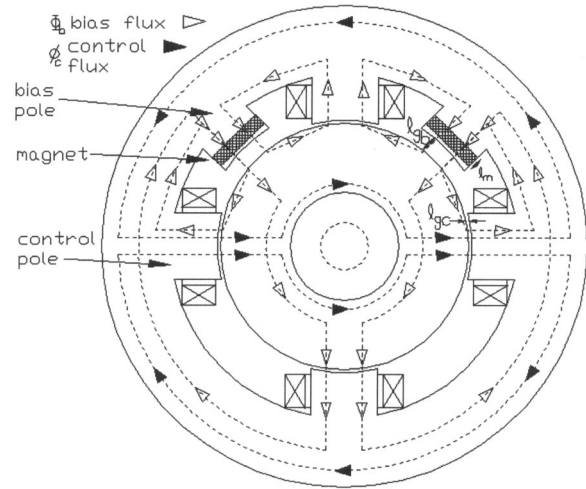


Fig. 2 Bias pole bearing that can support a constant gravity load with permanent magnet flux

take up space on the rotor and reduce the amount of controllable force that can be applied. Figure 1 shows an eight pole symmetric version of this type of bearing with bias poles.

The permanent magnets in all the bias poles are oriented to push flux into the rotor. The flux returns out through the control poles. The coils on the control poles can add or subtract a control flux to the bias flux. Generally control coils on opposing poles separated by one hundred and eighty degrees are wired in series. This way the control flux can add to the bias flux on one side of the rotor and subtract from the bias flux on the other side. A controllable net force on the rotor is then produced. The force adding and force subtracting poles do not have to be on exact opposite sides.

In cases where a constant side load needs to be supported, the bias poles can be placed on that side as shown in Fig. 2. The bias poles on one side can have a smaller area at the gap to concentrate the bias flux density and the bias force on that side. The permanent magnet can also be placed between a split control pole as shown in Fig. 3, or a split magnet can be placed beside the coils of single control poles. In all of these cases the magnetic circuit and performance equations are very similar. Specific details will be presented in the next sections for the eight pole symmetric bearing of Fig. 1(a). This will allow for a direct comparison between the eight pole bearing with four poles containing permanent magnets and the eight pole electrically biased heteropolar bearing of Fig. 1(b).

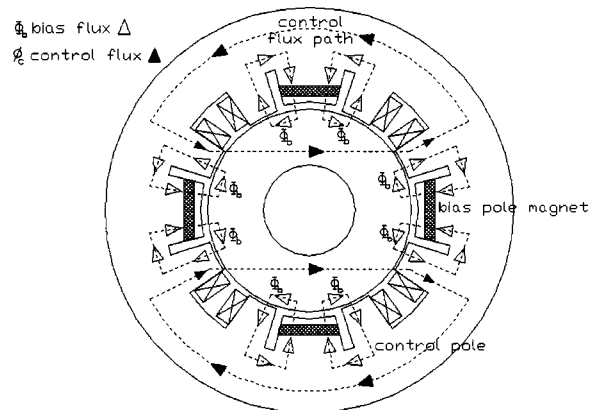
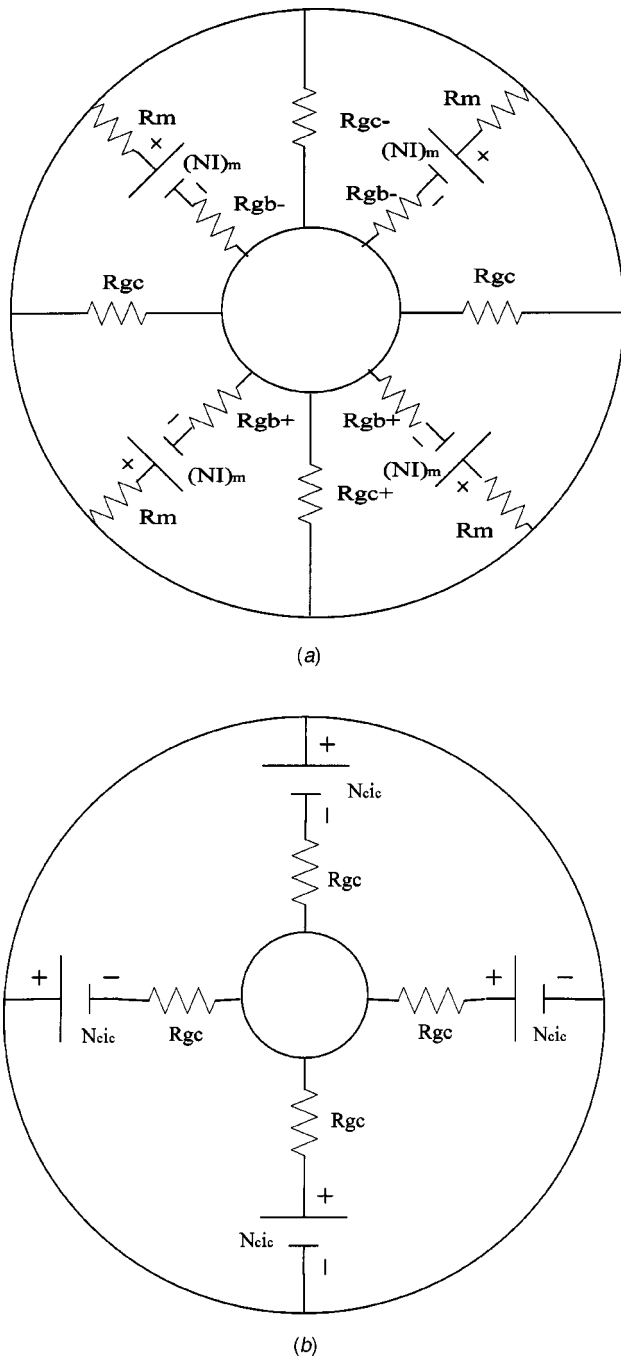


Fig. 3 Bias pole bearing with permanent magnet between split control poles



**Fig. 4 (a) Bias flux paths in an eight pole bias pole bearing (b) control flux paths in an eight pole bias pole bearing**

The bias pole bearing has two different gap reluctances: one for the gap under the bias poles, and one for the gap under the control poles. Both the area and the length of the bias pole gap may be different than that of the control pole gap. The bias flux path circuit for this bearing is shown in Fig. 4(a). The control flux path circuit is shown in Fig. 4(b). It has only four branches because the high reluctance of the magnet in each bias pole and the large bias pole air gap takes these poles out of the control flux circuit.

### 3 Actuator Characteristics

**3.1 Magnet Flux.** The bias flux,  $\Phi_b$ , is determined by the thickness of the permanent magnet. The thickness of the magnet can be calculated once the air gap thicknesses have been set. The

bias pole bearing is likely to have two different gap reluctances since it is advantageous to have a large gap under the bias pole to lower its contribution to the bearing position stiffness. The equivalent magnetomotive force (mmf),  $NI_m$ , required by the magnet can be determined from the circuit models, and for the bias pole bearing it is given by Eq. (1).

$$NI_m = \Phi_b(R_m + R_{gb} + R_{gc}) \quad (1)$$

In this equation  $R_m$  is the reluctance of the permanent magnet, and  $R_{gb}$  and  $R_{gc}$  are the reluctances of the gaps under the bias and control poles. The magnet mmf also depends on its thickness,  $l_m$ , and material properties as in Eq. (2).

$$NI_m = \frac{l_m B_o}{\mu_m} \quad (2)$$

Here  $B_o$  is the permanent magnet remanence flux density and  $\mu_m$  is its permeability.

Thus the required magnet length is as given by Eq. (3) assuming that poles, the magnet, and the air gaps all have the same cross section area for the flux.

$$l_m = \frac{\mu_m B_m (l_{gc} + l_{gb})}{\mu_m B_o - \mu_o B_m} \quad (3)$$

Here  $B_m$  is the flux density in the magnet.

The high energy and low permeability of NdFeB magnets enables them to be thin enough to be placed in the poles. For a 35 MGO magnet the relative permeability is 1.04 and the coercivity is 920000 A/m [26]. A bearing with a .635 mm gap (.025 in) under the control poles and a 3.175 mm gap (.125 in) under the bias poles would require a 12 mm thick (.47 in) magnet in each bias pole. The use of NdFeB magnets may limit the operating temperature to below 100 degrees centigrade [27].

**3.2 Load Capacity.** The bearing biased with magnets in four of the poles will have a lower load capacity per unit length because those four poles cannot contribute to the force. For this bearing the maximum force produced in the X' or Y' direction is given by Eq. (4) where  $F_{psat}$  is the force in a magnetically saturated pole. The maximum force produced by a conventional electrically biased heteropolar bearing is  $F_{ebsp}$  and given by Eq. (5).

$$F_{bpb} = 2 \cos(45^\circ) F_{psat} = 1.414 F_{psat} \quad (4)$$

$$F_{ebsp} = 2 \cos(22.5^\circ) F_{psat} + 2 \cos(67.5^\circ) F_{psat} = 2.613 F_{psat} \quad (5)$$

The load capacity for the bearing biased with magnets in the poles is only fifty-four percent of an electrically biased heteropolar bearing, as shown by Eq. (6). The load capacity in the X' or Y' direction is for both bearings  $2 \cos(45^\circ)$  times higher than in the X or Y direction. Therefore the ratio does not change.

$$\frac{F_{bpb}}{F_{ebsp}} = \frac{1.414}{2.613} = .54 \quad (6)$$

If required, this load capacity reduction may be compensated by increasing the laminate stack length. Equation (6) is a conservative estimate favoring the conventional heteropolar design. The control poles of the permanent magnet biased bearing can be larger in area than in the heteropolar design by using the coil space not required with the permanent magnet bias poles.

**3.3 Current Stiffness.** The current stiffness ratio for the two bearing types can also be calculated. The control flux,  $\phi_c$ , is proportional to the control current as given by Eq. (7).

$$\phi_c = \frac{N_c i_c \mu_o A_{gc}}{l_{gc}} \quad (7)$$

Here  $N_c$  is the number of turns in each control coil and  $i_c$  is the peak amplitude of the control current. The area of the gap under the control pole is,  $A_{gc}$ , and the gap length is  $l_{gc}$ .

The force on the rotor due to two poles separated by one hundred and eighty degrees is  $\Delta F_p$  given by Eq. (8).

$$\Delta F_p = \frac{2\Phi_b \phi_c}{\mu_o A_{gc}} \quad (8)$$

The current stiffness is defined by Eq. (9) where  $F_{net}$  is the combination of all poles working in harmony to give the maximum force.

$$K_i = \frac{dF_{net}}{di_c} \quad (9)$$

Substituting the force  $\Delta F_p$  for  $F_{psat}$  in Eq. (4) and Eq. (5) and utilizing the current stiffness definition, Eq. (9), it follows that the current stiffness of both bearings is given by Eq. (10) and Eq. (11) in the X or Y direction.

$$K_{i\_bpb} = \frac{2\Phi_b N_c}{l_{gc}} \quad (10)$$

$$K_{i\_ebsp} = \frac{2\Phi_b N_c}{l_{gc}} 2 \cos(22.5) = \frac{3.696\Phi_b N_c}{l_{gc}} \quad (11)$$

In these equations  $K_{i\_bpb}$  is the current stiffness of the permanent magnet biased bearing and  $K_{i\_ebsp}$  is that of the electrically biased bearing. Thus the current stiffness of bearing with bias poles is only fifty-four percent of the electrically biased single plane bearing as in Eq. (12). This may again be compensated by increasing the laminate stack length.

$$\frac{K_{i\_bpb}}{K_{i\_ebsp}} = \frac{2.000}{3.696} = .54 \quad (12)$$

This ratio is also the same in the X or Y direction as in the X' or Y' direction.

**3.4 Stator Efficiency.** The efficiency of these bearings is inversely proportional to the unwanted power loss. Causes of this power loss include hysteresis, eddy currents, and resistive losses in the coils. Hysteresis and eddy current losses may be significant, and eddy current losses can be especially severe at high rotor speeds [7]. However, they are beyond the scope of this paper. The efficiency considered here is based on only the coil resistive loss. In particular,  $F_{bpb}/P_{bpb}$ , is the efficiency ratio used for this study of the bias pole bearing, where  $F_{bpb}$  is the maximum force of the bearing and  $P_{bpb}$  is the corresponding resistive power consumed in the electric coils.

The ratio of load capacity to electrical power dissipated in the coils is favorable for permanent magnet biased bearings. The  $i^2R$  resistive power loss in the coils,  $P_{ebsp}$ , of an electrically biased single plane bearing is given by Eq. (13) where  $I_b$  is the dc bias current,  $R$  is the coil resistance and  $np$  is the number of active poles with coils.

$$P_{ebsp} = \left( I_b^2 + \frac{1}{2} i_c^2 \right) R \cdot np \quad (13)$$

The power required depends on the chosen ratio of  $I_b : i_c$ . A controller which maintains stability and minimizes power has been presented by Meeker and Maslen [28], for a heteropolar bearing. Lee, Hsiao, and Ko discuss choosing the ratio in terms of improving slew rate response in permanent magnet biased heteropolar bearings [29]. In this paper, we chose  $I_b = i_c$  as a baseline for comparison with the acknowledgement that the bearing efficiency will depend on the controller sophistication as well as the bearing geometry. The power lost as heat in the coils is given by Eq. (14).

$$P_{ebsp} = 1.5 i_c^2 R \cdot np \quad (14)$$

The permanent magnet biased bearings need no bias current. The bearing with bias pole magnets also has half as many coils. For this bearing the power required,  $P_{bpb}$ , is given by Eq. (15).

$$P_{bpb} = \frac{1}{2} i_c^2 R \cdot \frac{1}{2} np \quad (15)$$

The bearing with bias poles loses one sixth the power in the coils. This is shown by Eq. (16).

$$\frac{P_{bpb}}{P_{ebsp}} = \frac{\frac{1}{4}}{1.5} = \frac{1}{6} \quad (16)$$

The permanent magnet biased bearing improvement in power consumed compensates for the loss in load capacity. This is shown by Eq. (17). The bias pole bearing has a load capacity to power loss ratio that exceeds that of the electrically biased single plane bearing by a factor of 3.24.

$$\frac{F_{bpb}/P_{bpb}}{F_{ebsp}/P_{ebsp}} = 54.6 = 3.24 \quad (17)$$

**3.5 Position Stiffness.** The position stiffness of the bearing biased with magnets in the bias poles is lowered by the long length of the magnets and large air gap under the bias poles which makes for a small change in the bias flux with small movements of the rotor. When the rotor is moved slightly off center by an amount  $\Delta x$ , then there is only a significant change in the flux in the relatively short gap under the control poles. The change in flux under these poles due to a small displacement of the rotor is given by Eqs. (18–19) where  $\Phi_b$  is the bias flux with the rotor centered,  $\Phi_{bgc+}$  is the bias flux in the gap which is lengthened by the rotor displacement, and  $\Phi_{bgc-}$  is the bias flux in the gap which is shortened.

$$\Phi_{bgc+} = \Phi_b \frac{l_{gc}}{l_{gc} + \Delta x} \quad (18)$$

$$\Phi_{bgc-} = \Phi_b \frac{l_{gc}}{l_{gc} - \Delta x} \quad (19)$$

The force,  $F_{bpb\Delta x}$ , due to a small displacement of the rotor in the X or Y direction is then given by Eq. (20).

$$F_{bpb\Delta x} = \left( \frac{\Phi_{bgc+}^2}{2\mu_o A_{gc}} - \frac{\Phi_{bgc-}^2}{2\mu_o A_{gc}} \right) \quad (20)$$

Taking the limit with very small displacement,  $\Delta x$ , gives the position stiffness for the bias pole bearing as shown in Eq. (21).

$$K_{p\_bpb} = \frac{-2\Phi_b^2}{\mu_o A_{gc} l_{gc}} \quad (21)$$

In some cases, the position stiffness of the permanent magnet biased bearing may be used to advantage to support a constant side load with very little control current or power consumption. If the magnitude and direction of the static load is known, then the bias flux density may be used to support most or all of it by establishing a controller target position offset from center, in the opposing direction. The counteracted side load,  $F_{sl}$ , is proportional to the position stiffness and target offset as in Eq. (22).

$$F_{sl} = K_{p\_bpb} \Delta x \quad (22)$$

Another approach is to construct a bias pole that tapers down in the iron between the magnet and air gap. That will increase the magnetic attraction toward that pole since, as Eq. (20) indicates, the force is inversely proportional to the area. The static load capacity may not be a design concern for the radial magnetic bearings if the machine operates in a zero-g environment, e.g., satellite based flywheels or momentum wheels.

Following a similar procedure as Eq. (18)–(22), the position stiffness of the electrically biased single plane bearing,  $K_{p\_ebsp}$  is determined to be Eq. (23).

$$K_{p\_ebsp} = \frac{-2\Phi_b^2(1 + \cos^2 45)}{\mu_o A_{gc} l_{gc}} = \frac{-3\Phi_b^2}{\mu_o A_{gc} l_{gc}} \quad (23)$$

Equations (21) and (23) allow a direct comparison to be made between the position stiffness of the bias pole bearing and electrically biased single plane bearing. For the comparison, the bias flux density under all the C core poles of the electrically biased single plane bearing is made equal to the bias flux density under the poles of the bias pole bearing. Also for the comparison, the pole area and gap length dimensions of the control poles of the bias pole bearing and all the poles the electrically biased bearing are equal. The position stiffness of the permanent magnet bearing is two thirds that of the electrically biased single plane bearing as in Eq. (24). The position stiffness in the X' or Y' directions for both bearings is the same as in the X or Y direction, so the ratio given by Eq. (24) is still the same.

$$\frac{K_{p\_bpb}}{K_{p\_ebsp}} = \frac{2}{3} \quad (24)$$

**3.6 Achievable Bearing Stiffness.** The relative achievable stiffnesses presented next are based on the relative current and position stiffnesses derived previously. Equation (25) shows the achievable stiffness of the electrically biased single plane bearing as a reference. As a conservative estimate the achievable stiffness of the bias pole bearing relative to that of the electrically biased single plane bearing is given by Eq. (26).

$$K_{a\_ebsp} = K_{i\_ebsp} K_{pa} K_c + K_{p\_ebsp} \quad (25)$$

$$K_{a\_bpb} = .54 K_{i\_ebsp} K_{pa} K_c + \frac{2}{3} K_{p\_ebsp} \quad (26)$$

Here  $K_{a\_ebsp}$  is the achievable stiffness of the electrically biased single plane bearing and  $K_{a\_bpb}$  is the achievable stiffness of the permanent magnet biased single plane bearing. The controller gain is  $K_c$ . The achievable stiffness of the permanent magnet biased bearing is actually a little less than half that of the electrically biased bearing. This follows from comparing Eqs. (25) and (26) and considering that the position stiffness has a negative value.

#### 4 Comparison to Finite Element Model Predictions

A three dimensional finite element model of an eight pole bearing was created. The alternating four poles contained permanent magnets 12 mm (.47 in) thick. They were 35 MGO NdFeB magnets with a remanence of 1.22 T and a coercivity of 920000 A/m. The bearing cross section area through the poles, the rotor, and the circumferential paths were all equal. The air gap between the rotor and the active poles was .635 mm (.025 in). The air gap between the rotor and the bias poles was 3.175 mm (.125 inch). The outer diameter of the bearing was 17.8 cm (7 in), and the rotor outer diameter was 10.2 cm (4 in). The bearing thickness was 38.1 mm (1.5 in). Figure 5 shows the three dimensional finite element model of the bearing.

The finite element model was used to calculate the flux distribution due solely to the permanent magnets in the bias poles, with the control coils carrying zero current as is shown in Fig. 6(a). Similarly with the control coils energized to produce a force directly in the X direction, and with “demagnetized” permanent magnets modeled simply as a material with a relative permeability of 1.04, the FEA model calculated the control flux distribution shown in Fig. 6(b). The control flux to pull the rotor in the X' direction is shown in Fig. 6(c).

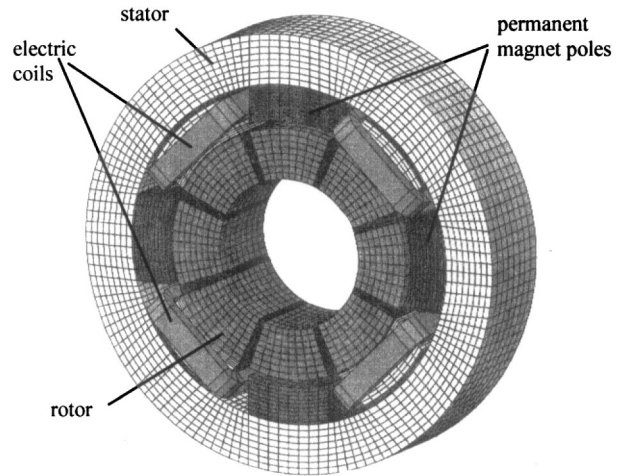


Fig. 5 Finite element model of bearing with permanent magnets in alternating poles

To calculate the current stiffness, position stiffness, and load capacity of the bearing with the finite element model, the combined flux distribution of the coils and permanent magnets was calculated. This is shown in Fig. 7.

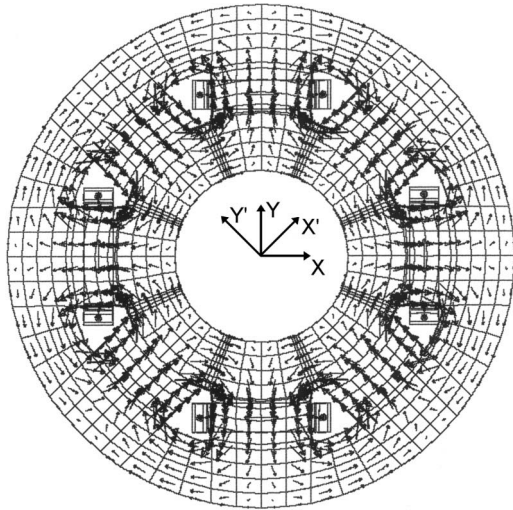
First, the finite element model was used to check that the equations for the load capacity and stiffness were derived correctly. In the model, the relative permeability of the rotor and stator were set to 100,000 to simulate the negligible reluctance of the metal path assumed by the circuit model. The rotor was set in the exact center. The bias flux was calculated from the finite element model analysis by integrating the flux density across the control gap area. The control flux was determined the same way. These values for the control and bias flux were substituted into Eq. (4), Eq. (8), Eq. (11) and Eq. (21). The fringe factor was set to one since the gap fluxes were known. This gave numerical values for the load capacity and stiffness partly based on the derived equations. Then, the finite element model was adjusted by displacing the rotor .076 mm (.003 in.) in the Y' direction. The force on the rotor was calculated from this model using maxwell stress tensor integration and the stiffnesses were calculated directly from the X' and Y' components of this force.

The stiffness and load capacity determined from the maxwell stress tensor integration and the circuit equations are compared in Tables 1–3. The difference between the predictions did not exceed four percent.

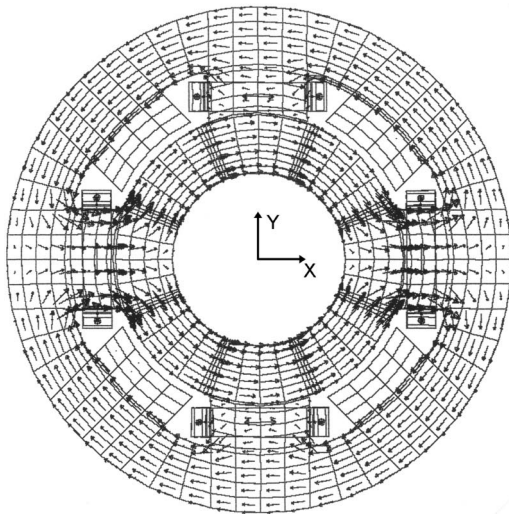
A second comparison was made. It showed the effects of flux saturation, actual alloy permeability, gap fringing, and leakage around the permanent magnet. The bias and control flux calculated from the finite element model were not substituted into the circuit model equations to calculate the load capacity and stiffness. Instead, the bias flux used was from the circuit model Eq. (3), and the control flux was calculated from circuit model Eq. (7). The load capacity and stiffness were calculated from the circuit models by substituting the circuit model predicted fluxes into the circuit model equations.

The fields and flux densities were calculated from a finite element model using a nonlinear BH curve for alloy Hyperco50A with a standard heat treatment [29]. The gap flux densities, the load capacity, and the current stiffness were calculated by an analysis with the rotor in the exact center of the model. The position stiffness was calculated with the rotor displaced .076 mm (.003 in) in the X' direction. Tables 4–8 compare the gap flux density, load capacity, and stiffness calculated from the finite element model analysis and the circuit model equations.

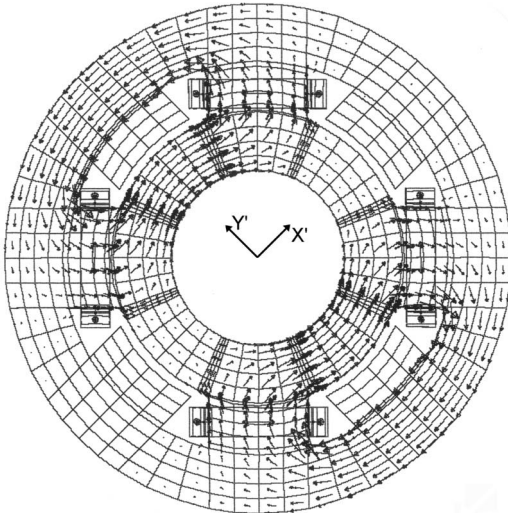
Several tables require clarification. Table 5 shows control fluxes used to calculate the current stiffness and load capacity. To mea-



(a)



(b)



(c)

Fig. 6 (a) Bias flux from permanent magnets in poles (b) control flux to pull rotor in X direction (c) control flux to pull rotor in X' direction

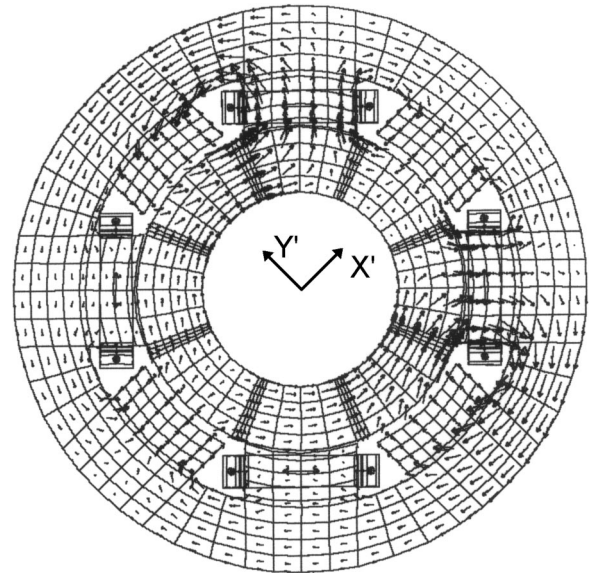


Fig. 7 Bias pole bearing with combined bias flux and control flux to pull rotor in the X' direction

Table 1 Position Stiffness in Y' direction.

1-D Equation	3-D FEA	Percent Difference
-1.961 MN/m	-1.957 MN/m	-.020
-11200 Lb/in	-11182 Lb/in	

Table 2 Current Stiffness in X' direction.

1-D Equation	3-D FEA	Percent Difference
456 N/A	441 N/A	-3.4
(102 Lb/A)	(99.2 Lb/A)	

Table 3 Load Capacity in X' direction.

1-D Equation	3-D FEA	Percent Difference
1436 N	1412 N	-1.7
(323 Lb)	(318 Lb)	

Table 4 Nonlinear Model Bias Flux Through Control Gap.

1-D Equation	3-D FEA	Percent Difference
.90 T	.704 T	-29

Table 5 Nonlinear Model Control Flux Density Through Control Gap.

1-D Equation	3-D FEA	Percent Difference
.09 T	.084 T	-7.2
.90 T	.73 T	-24.5

Table 6 Nonlinear Model Position Stiffness in Y' direction.

1-D Equation	3-D FEA	Percent Difference
-2.721 MN/m	-1.672 MN/m	-62.7
(-15540 Lb/in)	(-9555 Lb/in)	

**Table 7 Nonlinear Model Current Stiffness in X' direction.**

1-D Equation	3-D FEA	Percent Difference
537 N/A (121 Lb/A)	417 N/A (93.8 Lb/A)	-29

**Table 8 Nonlinear Model Load Capacity in X' direction.**

1-D Equation	3-D FEA	Percent Difference
2454 N (552 Lb)	1657 N (372 Lb)	-48

sure the current stiffness, a small control flux was used along with the bias flux. To measure the load capacity, the control current was set equal to that predicted by the circuit model to give an amount of control flux that would equal the bias flux. In that case, the flux density was high enough that the material saturation level was nearing, which lowered the amount of control flux produced.

The load capacity in Table 8 is predicted to be higher by the nonlinear finite element analysis than is shown in Table 3 for the linear analysis. This is because the control flux level used to calculate the value in Table 3 was set slightly less than the bias flux level to insure that the flux did not reverse in the gap, which was a presumption of the load capacity calculation based on the circuit model.

All the tables show that the values predicted by the finite element model are the lowest. Although the circuit models are useful as a conceptual tool, they have significant limitations. Lee, Hsiao, and Ko [30] found a similar discrepancy when using simple circuit models to calculate the performance of permanent magnet biased homopolar bearings.

Two approaches can be taken to bring the circuit model and finite element model predictions in closer agreement. One is to refine the circuit model to include the alloy reluctance, an estimate of gap fringing and permanent magnet leakage, and other factors as done by Meeker, Maslen and Noh [31]. This will lower the predicted values in the circuit model. The second approach is to refine the bearing geometry by determining the best lengths and areas of the bias and control pole air gaps, the best magnet dimensions, and make geometry improvements as done by Overstreet, Flowers, and Szasz for homopolar bearings [9]. This will raise the load capacity and stiffnesses. Both approaches could be the subject of further research and development.

## 5 Summary

A bearing using poles with permanent magnets dedicated solely to providing bias flux has been presented. The performance equations developed in this paper for the bearing show it has about half the load capacity, current stiffness, and displacement stiffness of an electrically biased heteropolar bearing of the same size and with the same total number of poles. The achievable stiffness is less than half that of the electrically biased bearing. The lower load capacity and stiffness may be increased by utilizing the additional pole area made available by one half the number of coils. Because it has half as many electric coils and uses no bias current, the bearing with permanent magnet poles needs only one sixth as much electric power to have the same bias flux as the electrically biased heteropolar bearing. The ratio of load capacity to power dissipated in the coil can be 3.24 times higher for this permanent magnet biased bearing. These conclusions were reached after deriving the performance equations for the bearing from bias flux and control flux circuit models which were confirmed by a three dimensional finite element analysis of the bearing. The finite element model also showed that improvements are needed in the circuit model in order to make accurate predictions of the bearing

parameters because of fringing, leakage, and magnetic saturation. Research is also necessary to develop a procedure for finding the best bearing geometrical parameters so that the bearing can achieve a performance as near as possible to its theoretical limit.

## Acknowledgments

The authors gratefully acknowledge the support provided for this work from Albert Kascak, Gerald Montague, Andy Provenza, and Raymond Beach of NASA Glenn (Grants NRA-99-GRC-2) and from Tom Calvert, Lyn Peterson, and Glenn Bell of the Navy NSWC (Grant ONR BAA97-030).

## References

- [1] Schweitzer, G., Bleuler, H., and Traxler, A., 1994, *Active Magnetic Bearings*, VDF Hochschulverlag AG an der ETH, Zurich.
- [2] Meeks, C. R., DiRusso, E., and Brown, G. V., 1990, "Development of a Compact, Light Weight Magnetic Bearing," *Proc. of the 26th Joint Propulsion Conference AIAA/SAE/ASME/ASEE*, Orlando.
- [3] Sortore, C. K., Allaire, P. E., Maslen, E. H., Humphris, R. R., and Studer, P. A., 1990, "Permanent Magnetic Biased Bearings—Design, Construction, and Testing," *Proc. of the Second International Symposium on Magnetic Bearings*, Tokyo, pp. 175–182.
- [4] Nataraj, C., and Calvert, T. E., 1998, "Optimal Design of Radial Magnetic Bearings," *Proc. of the Sixth International Symposium on Magnetic Bearings*, Cambridge, MA, pp. 296–305.
- [5] Grbesa, B., 1998, "Low Loss and Low Cost Active Radial Homopolar Magnetic Bearing," *Proceedings of the Sixth International Symposium on Magnetic Bearings*, Cambridge, MA, pp. 286–295.
- [6] Saari, J., and Lindgren, O., 1994, "Estimation of the Temperature Rise in High-Speed Electrical Machines with Magnetic Bearings," *Proc. of the Fourth International Symposium on Magnetic Bearings*, Zurich, pp. 571–576.
- [7] Kasarda, M. E. F., Allaire, P. E., Norris, P. M., Mastrangelo, C., and Maslen, E. H., 1998, "Experimentally Determined Rotor Power Losses in Homopolar and Heteropolar Magnetic Bearings," *Proc. of the 1998 International Gas Turbine & Aeroengine Congress & Exhibition*, Stockholm, 98-GT-317.
- [8] Lee, A., Hsiao, F., and Ko, D., 1994, "Analysis and Testing of Magnetic Bearing with Permanent Magnets for Bias," *JSME Int. J., Ser. C*, **37**(4), pp. 774–782.
- [9] Fan, Y., Lee, A., and Hsiao, F., 1997, "Design of a Permanent/Electromagnetic Magnetic Bearing-controlled Rotor System," *J. Franklin Inst.*, **334B**(3), pp. 337–356.
- [10] Overstreet, R. W., Flowers, G. T., and Szasz, G., 1999, "Design and Testing of a Permanent Magnet Biased Magnetic Bearing," *Symposium on Vibration of Rotating Structures and Systems for the 1999 ASME Design Technical Conferences (17th Biennial Conference on Mechanical Vibration and Noise)*, Las Vegas, pp. 1–8.
- [11] Fukata, S., Yutani, K., and Kouya, Y., 1998, "Characteristics of Magnetic Bearings Biased with Permanent Magnets in the Stator," *JSME Int. J., Ser. C*, **41**(2), pp. 206–213.
- [12] Jagannathan, S., 1991, "Analysis and Design of Magnetic Bearings," M.S. Thesis, University of Virginia.
- [13] Schmidt, E., Platter, T., and Springer, H., 1996, "Force and Stiffness Calculations in Magnetic Bearings—Comparison between Finite Element Method and Network Theory," *Fifth International Symposium on Magnetic Bearings*, Kanazawa, Japan, pp. 259–264.
- [14] Rockwell, R. D., Allaire, P. E., and Kasarda, M. E. F., 1997, "Radial Planar Magnetic Bearing Analysis with Finite Elements Including Rotor Motion and Power Losses," *Proc. of the 1997 International Gas Turbine & Aeroengine Congress & Exposition*, 97-GT-503.
- [15] Imlach, J., Blair, B. J., and Allaire, P. E., 1990, "Measured and Predicted Force and Stiffness Characteristics of Industrial Magnetic Bearings," *Joint ASME/STLE Tribology Conference*, Toronto, 90-Trib-70.
- [16] Fitro, R. L., Baun, D. O., Maslen, E. H., and Allaire, P. E., 1997, "Calibration of an 8-Pole Planar Radial Magnetic Actuator," *Proc. of the 1997 International Gas Turbine & Aeroengine Congress & Exposition*, Orlando, 97-GT-18.
- [17] Masayuk, Y., 1999, "Magnetic Bearing Device," Japanese patent 11101234A.
- [18] Nagahiko, N., 1986 "Magnetic Bearing," Japanese patent 61180019A.
- [19] Maslen, E. H., Allaire, P. E., Humphris, R. R., Noh, M. and Sortore, C. K., 1993, "Permanent Magnet Biased Active Magnet Bearings," *Proc. of Mag '93, Magnetic Bearings, Magnetic Drives, and Dry Gas Seals Conference and Exhibition*, Alexandria, pp. 117–128.
- [20] Lewis, D. W., Humphris, R. R., Maslen, E. H., Williams, R. D., 1994, "Magnetic Bearings for Pumps, Compressors, and other Rotating Machinery," U.S. Patent 5355042.
- [21] Yamauchi, A., Kuwahara, O., 2001, "Composite Type Electromagnet and Radial Magnetic Bearing," European Patent EP1072807A2.
- [22] Woodson, H. H., and Melcher, J. R., 1968, *Electromechanical Dynamics*, J. Wiley & Sons, New York.
- [23] Ida, N., and Bastos, J. P. A., 1997, *Electromagnetics and Calculation of Fields*, Springer, New York.
- [24] Vector Fields Limited, 1999, *Opera-3d Reference Manual*, Oxford, England.
- [25] Kenny, A., and Palazzolo, A. B., 2001, "Theory and Test Correlation for Lami-

- nate Stacking Factor Effect on Homopolar Bearing Stiffness,” *Proc. of the ASME Turbo Expo: Land, Sea, and Air, New Orleans*, 2001-GT-0294.
- [26] Dexter Magnetic Technologies, Inc, 2001, “Neodymium Iron Boron Standard Parts,” [www.dextermag.com/neo\\_parts.htm](http://www.dextermag.com/neo_parts.htm).
- [27] Gieras, J. F., and Wing, M., 1997, *Permanent Magnet Motor Technology Design and Applications*, Marcel Dekker, New York.
- [28] Meeker, D. C., and Maslen, E. H., 1996, “Power Optimal Solution of the Inverse Problem for Heteropolar Magnetic Bearings,” *Proc. of the Fifth International Symposium on Magnetic Bearings*, Kanazawa, Japan, pp. 283–288.
- [29] Carpenter Magnetic Alloys, 1995, Carpenter Technology Corporation, Carpenter Steel Division, Philadelphia, PA.
- [30] Lee, A., Hsiao, F., and Ko, D., 1994, “Performance Limits of Permanent Magnet Biased Magnetic Bearings,” *JSME Int. J., Ser. C.*, , **37**(4), pp. 783–794.
- [31] Meeker, D. C., Maslen, E. H., and Noh, M. D., 1996, “An Augmented Circuit Model for Magnetic Bearings Including Eddy Currents, Fringing, and Leakage,” *IEEE Trans. Magn.*, **32**(4), pp. 3219–3227.